

CHROMSYMP. 1627

HIGH-PERFORMANCE LIQUID CHROMATOGRAPHY OF AMINO ACIDS, PEPTIDES AND PROTEINS

XCII^a. THERMODYNAMIC AND KINETIC INVESTIGATIONS ON RIGID AND SOFT AFFINITY GELS WITH VARYING PARTICLE AND PORE SIZES

F. B. ANSPACH, A. JOHNSTON and H.-J. WIRTH

Department of Biochemistry and Centre for Bioprocess Technology, Monash University, Clayton, Victoria 3168 (Australia)

K. K. UNGER

Institut für Anorganische Chemie und Analytische Chemie, Johannes Gutenberg-Universität, 6500 Mainz (F.R.G.)

and

M. T. W. HEARN*

Department of Biochemistry and Centre for Bioprocess Technology, Monash University, Clayton, Victoria 3168 (Australia)

SUMMARY

In these investigations Cibacron Blue F3GA was immobilized on soft gels, porous silicas, and non-porous glass beads. Hen egg white lysozyme, human serum albumin and yeast alcohol dehydrogenase were used as adsorbates with the dye-affinity sorbents. Batch experiments with continuous monitoring of protein concentration were employed to evaluate thermodynamic and kinetic behaviour of these proteins in finite bath systems. The observed adsorption kinetic rates of interaction of the above proteins with each of the dye-affinity sorbents were found to decrease with increasing protein molecular weight. Equilibration times, in the batch experimental mode, of the adsorption of lysozyme on the dye-affinity sorbents varied from 20 s for the non-porous glass beads with a size range of 20–40 μm to more than 60 min in the case of a porous sorbent with a particle diameter of 100–300 μm and 60 nm pore size. Furthermore, equilibration times, which represent the overall adsorption rates incorporating all the non-equilibrium effects, increased with all affinity systems when adsorption took place in the non-linear portion of the isotherm. The most dramatic increase was observed when sorbents with relatively high protein size to pore size ratios, λ , were employed.

^a For Part XCI, see ref. 1.

INTRODUCTION

Economics, efficiency and practicality are some of the constraints dictating the search for novel chromatographic supports that exhibit high purification performance for proteins of industrial importance. In this regard, protein specific affinity chromatography or ion-exchange and other forms of electrostatic chromatography, which exploit differences in biological specificity or surface charge anisotropy of proteins, have the greatest potential in the isolation of the desired protein^{2,3}. The large-scale purification of commercially important proteins to the high degree of purity necessary for pharmaceutical products requires integration of each purification stage. Research-based information is thus essential permit accurate prediction of the mass transport and biological activity behaviour of the solute under various operational conditions.

Development of methods for accurate prediction of the overall mass-transfer resistances associated with the chromatographic separation of proteins, which from practical experience are not comparable to those observed with low-molecular-weight compounds, require the evaluation of a complex family of parameters which describe the large-scale adsorption and elution behaviour of proteins⁴⁻⁶. Most mathematical models earlier used for this evaluation do not account for the time course of mass-transfer resistances within and around the stationary phase particles, yet it is established experimentally that the transport of macromolecules in the pores of the sorbent is a slow process^{7,8}. Other studies on large-scale ion-exchange chromatography from this and other laboratories have also shown that the near-equilibrium hypothesis is often untenable in the overload mode^{9,10}.

The work described in the present investigations was aimed at elucidating some aspects associated with dye-affinity chromatography. In this respect, the adsorption and elution of different proteins, *i.e.* hen egg white lysozyme, human serum albumin, and alcohol dehydrogenase (yeast) from Cibacron Blue F3GA, immobilized on different soft and rigid chromatographic supports, was evaluated by using batch adsorption techniques analogous to the experimental set-up described by Chase⁵ and Arnold *et al.*¹¹. Overall rates of adsorption were determined and the adsorption characteristics compared at approximately 10% and 60% of the saturation of the sorbents.

THEORY

Factors controlling the thermodynamics in batch adsorption

The adsorption of a protein on an affinity sorbent relies on the affinity interaction, often described simply by the equilibrium relationship (eqn. 1), with the assumption that a single-site, homogeneous interaction occurs between the protein, P, and the ligand, L, and that non-specific interactions promoted by the support are absent. This relationship then takes the form



where k_1 and k_2 are the forward and reverse reaction rate constants. The rate of adsorption, as derived from eqn. 1, is then given by

$$\frac{dq}{dt} = k_1 c (q_m - q) - k_2 q \quad (2)$$

where c is the concentration of the solute in the mobile phase (bulk solution), q the concentration of the solute adsorbed on the affinity sorbent, and q_m the maximum capacity of the sorbent, representing the accessible concentration of immobilized ligands. When equilibrium exists throughout the system, the rate dq/dt is zero and eqn. 2 can be simplified to

$$q^* = \frac{q_m c^*}{K_d + c^*} \quad (3)$$

where K_d represents the dissociation constant. If it is assumed that only one type of interaction takes place, eqn. 3 describes the equilibrium isotherm, which has the same shape as isotherms reported more than 70 years ago by Langmuir for the adsorption of gases on solid phases¹².

These equations represent a simplistic case of protein adsorption. They describe a totally specific affinity of the protein, P, for the ligand, L. The results of the present study highlight the important practical reality that most, if not all, sorbents function as heterogeneous surfaces in terms of their structure and adsorption reactivities. Furthermore, the data are also consistent with the protein solute itself undergoing conformational changes and secondary chemical equilibria upon binding or in solution. This behaviour leads to further changes in sorbent reactivity which deviate from the simple equilibrium balance described above. In designing any process operation, attempts are made to minimize these non-idealities, but as is demonstrated in the present study it is not sufficient to presume that their effects are negligible or that their participation can be disregarded in the adsorption phenomenon.

Factors controlling the kinetics in batch adsorption

Typical analytes in affinity chromatography are large molecules with small diffusion coefficients. Because of their size and mainly globular shape the free diffusivity (intrinsic diffusivity), D_m , of proteins can be described by the modified Stokes-Einstein equation introduced by Young *et al.*¹³. The effective diffusivity, D_p , of a solute in a porous solid is related to its free diffusivity and the porosity of the solid and may be a much smaller value, when the ratio, λ , of the molecular size of the protein to the pore size is not negligible¹⁴. Additionally, when the ratio λ becomes large ($0.1 < \lambda < 1$), the reaction rate may be limited by rotational masking due to the highly specific adsorption step in affinity chromatography that often requires the appropriate orientation of the solute before adsorption on the affinity sorbent¹⁴. Similar behaviour has also been described for ion-exchange and hydrophobic interaction sorption of proteins^{15,16}. Detailed descriptions of restricted diffusion and rotational masking have also been provided by Smith and Fournier^{17,18}, and Yau *et al.*¹⁹. Besides the choice of the protein solute, the selection of the ligand and the sorbent matrix, in terms

of their physical and chemical characteristics, require adequate definitions if data derived from model studies are to be of generic utility.

Selection of model affinity chromatographic systems

In the present studies, the adsorption behaviour of three proteins with 11 different supports to which Cibacron Blue F3GA had been covalently immobilized, has been evaluated. The criteria used for the selection of the model protein, ligand and sorbent systems is indicated below.

Proteins. To investigate the effect of mass transport limitations on the overall adsorption, lysozyme (EC 3.2.1.17), human serum albumin (HSA), and alcohol dehydrogenase (ADH) (EC 1.1.1.1) were chosen as representative of proteins having different molecular weights yet exhibiting different interaction mechanisms with Cibacron Blue F3GA. The protein ADH was chosen as representative of a large protein having a binding rate which should be diffusion controlled. Further, the immobilized triazine dye can behave as a biomimetic ligand capable of mimicking the interactions of the specific cofactor with the reduced nicotinamide-adenine dinucleotide (NADH)-binding site. In contrast, the rate at which lysozyme binds may be not only diffusion but also kinetically controlled whilst the interaction was anticipated to be surface directed. The molecular dimensions of HSA lie between ADH and lysozyme with the interaction again surface directed to each domain. The particular molecular characteristics of these three proteins are summarized in Table I.

Ligand. Biomimetic affinity chromatography based on immobilized triazine dyes is a well-established technique for the purification of proteins. The type of dye ligand employed in the affinity system will determine the nature of the binding to numerous classes of proteins either in a highly specific mode, where the chemical structure of the immobilized dye mimics the cofactor binding to specific allosteric or active sites of various enzymes²⁰, or in a less specific mode, where oppositely charged ionic groups at the protein surface and within the chemical functionality of the dye as well as hydrophobic binding sites between the two interacting species induce very strong adsorption of several classes of proteins^{21,22}. For this study, Cibacron Blue F3GA was selected because it is predominantly used as a reactive dye and because its structure and chemical composition (in terms of impurity composition also) are well

TABLE I
MOLECULAR DIMENSIONS AND PROPERTIES OF PROTEINS

<i>Protein</i>	<i>Molecular weight ($\cdot 10^3$ daltons)</i>	<i>Accessible surface area ($\cdot 10^8$ m²)^a</i>	<i>Diameter (nm)^b</i>	<i>Isoelectric point</i>
Hen egg white lysozyme	14.4	6.8	2.73	11.0
Human serum albumin	67	18.3	8.35	4.4–4.8
Alcohol dehydrogenase	148	31.1	10.2	8.1–9.3

^a Taken from Janin⁴².

^b Taken from Travers and Church⁴³.

known²³. Furthermore, Cibacron Blue F3GA immobilized on various soft gel and modified silica gel chromatographic supports exhibits similar chromatographic characteristics^{24,25} as an affinity sorbent. The similarity shared by these different sorbents in terms of overall selectivity is important if their adsorption characteristics are to be adequately discriminated.

Stationary phases. Cost-effective preparative separation of complex biological mixtures by any chromatographic procedure aims at (i) high mass recovery, (ii) maintenance of biological activity, (iii) high resolution, (iv) high peak productivity and capacity and (v) short separation time. Thus, considerable effort has been devoted by a number of research groups over the past several years to preparing tailor-made sorbents based either on soft gels (*i.e.* new modifications of agarose, dextrans, polyacrylamide, trishydroxymethylpolyacrylamide supports) or on rigid silicas as well as the new polymer-based hybrid-clad inorganic supports. These new sorbents have enlarged pore diameters that freely accommodate proteins with molecular weights of 200 000 and more with average pore diameters of 30–600 nm and particle sizes of 10–150 μm . Typically, such matrices are intended for large-scale purification.

An alternative approach to preparative isolation of proteins is the use of high-performance non-porous packing materials similar to those introduced by us in 1984²⁶. These matrices were initially designed as improved biospecific affinity sorbents in the analytical mode, but have been subsequently adapted to all modes of affinity chromatography²⁵, including dye–ligand affinity²⁴ and immunoaffinity chromatography²⁷. Our investigations have demonstrated much more favorable mass transport and adsorption/desorption kinetic behaviour with these non-porous sorbents.

Finally, a group of stationary phases, based on porous or non-porous fibres, chemically modified to permit their use in biospecific affinity adsorption, can also be considered. Such stationary phases have attracted some attention in recent years (*cf.*, *e.g.*, Wikström and Larsson²⁸). In the present study, however, only particulate systems have been examined.

EXPERIMENTAL

System conditions

The equilibration and adsorption buffer was 50 mM Tris \cdot HCl, adjusted to pH 7.8, for all systems. With the HSA and lysozyme adsorption studies in finite baths, two experiment protocols were performed, one with the buffer mentioned above and the second with 0.5 M NaCl, added to the buffer solution. Because of the effect on the binding characteristics of these two proteins with and without salt present in the buffer with the various affinity sorbents, another set of data was generated to validate the binding characteristics following regeneration. In the regeneration cycle, the gels were suspended 3 times in the buffer described above, containing 2.5 M KSCN, and incubated for at least 3 min in order to allow the proteins to diffuse out of the porous matrix. In the case of very low adsorption kinetics, the incubation time was increased up to 15 min. After regeneration, the gels were re-equilibrated in the working buffer by washing the gel 5 times with the 2.5 M KSCN solution in a Büchner funnel.

Chromatographic supports

Soft gel chromatographic supports, such as Fractogel HW 55 (S), Fractogel HW

65 (F), and Fractogel HW 75 (F), were obtained from Merck (Darmstadt, F.R.G.), Trisacryl GF 2000 from Reactifs IBF (Villeneuve la Garenne, France), Cellufine GC 200 Medium and Cellufine GC 700 Medium from Amicon (Danvers, MA, U.S.A.), and Sepharose 4B, Sepharose CL6B, and Blue Sepharose CL6B from Pharmacia (Uppsala, Sweden).

The porous silica-based supports which were studied were Spherosil (Type X0B030) from Rhône-Poulenc (Usine de Salindres, France), and Nucleosil 300-2540 from Macherey Nagel (Düren, F.R.G.). Non-porous glass beads were a gift from Polters-Ballotini, Kirchheimbolanden, F.R.G. Characteristic parameters of the chromatographic supports are summarized in Table II.

Chemicals

3-Mercaptopropyltrimethoxysilane (MPS) and 1,6-lutidine were obtained from EGA (Steinheim, F.R.G.). Tris, hen egg white lysozyme (EC 3.2.1.17, dialysed and lyophilized) and ADH (EC 1.1.1.1, crystallised and lyophilized) from baker's yeast were purchased from Sigma (Sydney, Australia). Cibacron Blue F3GA was obtained from Serva (Heidelberg, F.R.G.). HSA (chromatographically isolated, containing 250 mg/ml protein, 85–130 mM sodium chloride and 40 mM sodium octanoate) was a gift from the Commonwealth Serum Laboratories (Melbourne, Australia).

Dialysis of HSA solution

In order to preclude undesirable absorption of the detergent (sodium octanoate) present in the stock protein solution to the Cibacron Blue F3GA-immobilized affinity sorbents, the HSA solution was diluted to a final concentration of 50 mg/ml protein and dialysed against 50 mM Tris · HCl (pH 7.8) at 277 K by changing the buffer 4 times at 8 h intervals.

TABLE II
CHARACTERISTIC PARAMETERS OF CHROMATOGRAPHIC SUPPORTS

Support	Particle size d_p (μm)	Operating range of native sorbent ($\cdot 10^3$ daltons)	Pore size D_{p50} (nm)	Specific surface area (m^2/ml)
<i>Soft gels</i>				
Fractogel HW 55 (S)	25–40	1–900		
Fractogel HW 65 (F)	32–63	40–4500		
Fractogel HW 75 (F)	32–63	500–45 000		
Trisacryl GF 2000	40–80	120–15 000		
Cellufine GC 700	45–105	10–120		
Cellufine GC 200	45–105	10–400		
Sepharose 4B	45–165	80–20 000		
Sepharose CL6B	40–165	10–5000		
<i>Silica gels and glass beads</i>				
Spherosil X0B030	100–300		60	50
Nucleosil 300-2540	25–40		30	100
Glass beads fraction 4	20–40		—	0.19 ^a

^a Calculated from the geometric surface area, assuming a density for glass of 1.9 g/ml.

Preparation of protein solutions

Solutions of lysozyme and ADH were prepared daily by dissolving the protein of interest in the appropriate buffer to a final concentration between 19 and 21 mg/ml. Except for ADH, which was prone to precipitation during filtration, all protein solutions were filtered through 0.44- μm pore size filters to remove undissolved material.

Preparation of MPS-activated silicas

An amount of 5 g of either Spherosil X0B030 or Nucleosil 300 was suspended in 50 ml water (pH 3.5, adjusted with 0.01 *M* HNO_3). The pH was controlled and readjusted if necessary, and an equimolar quantity of MPS was added to the silica suspension, calculated on the basis of the specific surface area of the total amount of silica present, and an assumed amount of 8 μmol hydroxyl groups per m^2 of surface of the corresponding silica. The reaction vessel was evacuated to 2000 Pa, sonicated in an ultrasonic bath for 10 min, and then heated to 363 K for 3 h with stirring, essentially as described by Regnier and Noel²⁹. After it had cooled, the derivatized silica suspension was neutralized by suspending the modified silica in water and filtering several times. Subsequently, the MPS-silica was suspended 3 times in both toluene and chloroform and filtered.

Preparation of MPS-activated non-porous glass beads

In order to obtain particles of narrower particle-size distribution than the original range of 2–40 μm , the glass beads were suspended in water and four fractions (2–5, 5–10, 10–25, and 20–40 μm , determined by microscopic analysis) were separated by sedimentation. Only fraction 4 was used for the bath experiments, whilst fractions 2 (5–10 μm), 3 (10–25 μm) and 4 (20–40 μm) were selected for fundamental chromatographic studies. The glass beads were then suspended in 5 *M* HCl and shaken for 12 h at 323 K in order to remove surface-bound impurities, such as iron, which had been previously shown to be present. In addition, the use of 5 *M* HCl permitted surface-bound aminopropyl groups, covalently attached to the glass (as specified by the manufacturer), to be also removed. The glass beads were washed extensively with water, filtered, and dried in the presence of self-indicating silica gel. Subsequently, 5 g of the glass beads were suspended in 40 ml water (pH 3.5, adjusted with 0.01 *M* HNO_3), 0.3 g MPS (excess) were added, and the suspension was shaken for 2 h at 363 K. The washing procedure was the same as that described above for porous silicas. Due to the relatively high concentration of MPS compared to the surface area of the non-porous glass beads, parts of the surface may have been covered by polymerised silane molecules which had been added in excess. The high silane concentrations were used because very little binding of the silane occurred when a concentration of silane equivalent to surface-located silanol groups was used initially. To avoid polymerization, which can limit the diffusional characteristics of the sorbents, further optimization of this reaction procedure is necessary.

Purity of Cibacron Blue F3GA

According to Hanggi and Carr³⁰, most of the commercially available triazine dyes are very heterogeneous and often contain only a small percentage of the dye of interest. To survey the purity of triazine dyes which had been previously used for

various purifications, a rapid chromatographic test was performed with a Zorbax ODS column (250×4.6 mm I.D.) and a 15-min gradient of acetonitrile (0–80%) at a flow-rate of 1.5 ml/min. A photo diode-array detector, coupled in series with a second detector set at 610 nm, displayed impurities either as single peaks or indicated their presence as part of the peak broadening of the major component of almost all of the Procion dyes. This analysis showed only a single peak for the Cibacron Blue F3GA preparation used in this study. This was in accordance with the product information from Serva, who guaranteed a purity of 85–90%, buffer salts being the major contaminant.

Immobilization of Cibacron Blue F3GA

The modified silicas with immobilized mercapto-group functionalities were suspended in 100 mM Na_2CO_3 (pH 8)–0.5 M NaCl, containing Cibacron Blue F3GA, according to the procedure described by Small *et al.*³¹ for agarose-based gels. The reaction was carried out at 333 K by shaking the silica suspension for 12 h. The immobilized dye sorbents were washed by filtration or centrifugation and suspended several times in 50 mM Tris · HCl (pH 7.8) until the supernatants were colorless.

The reaction buffer for the soft gels was 100 mM Na_2CO_3 (adjusted to pH 9)–0.5 M NaCl. The soft gels were washed several times with the reaction buffer and filtered in order to remove chemicals added for stabilization of these sorbents. The moist gel (10 g) was suspended in 30 ml of the reaction buffer, and 150 mg Cibacron Blue F3GA were added. The reaction was carried out at 333 K (313 K for the Sepharose 4B support, since a maximum temperature of 313 K had been recommended³²), and the reaction vessels were shaken for 24 h.

Procedure for bath experiments

Bath experiments were performed by using the experimental set-up illustrated in Fig. 1. When soft affinity sorbents were used, between 0.3 g and 1 g (dried by drawing air through a sintered filter; 2 min for Fractogels, 10 min for other soft gels) of the gel were suspended in 20 ml buffer. When silica-based affinity sorbents were employed, between 0.2 g and 0.5 g of the completely dried gels were suspended in 20 ml buffer. To ensure complete penetration of the buffer solution into the pores of the affinity sorbents, reduced pressure (2000 Pa) was applied to the bath for 5–10 min prior to the experiments in order to remove air from the pore system. Complete mixing was

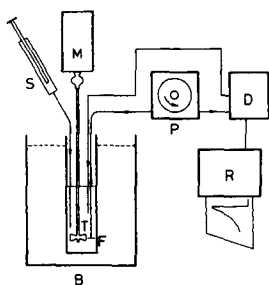


Fig. 1. Schematic diagram of experiment set-up of bath experiments. B = thermostatic bath, D = detector set at 280 nm, F = filter, P = peristaltic pump, R = chart recorder, S = HPLC syringe, T = continuously stirred tank (CSTR).

achieved with a turbine-blade stirrer, accommodating three blades, and operated with a rotary motor at 1100–1200 rpm. The adsorption apparatus was placed in a water bath thermostated at 308.5 K. A peristaltic pump continuously withdrew samples from the adsorption bath at a flow-rate of 1 ml/min, through a detector, set at 280 nm, back into the apparatus to keep the total volume constant. The protein concentration was monitored on a chart recorder connected to the detector. The detector was calibrated for each protein at different concentrations to allow accurate measurement of absolute protein concentrations. The dead volume of the system was kept to a minimum by using a tubing of 0.5 mm I.D. A filter with 12- μ m gauze was placed at the end of the inlet (suction) tubing to prevent the particles from passing through the detector cell.

After a steady state had been achieved, a sample of protein solution of known concentration and volume was injected into the apparatus with a high-performance liquid chromatography syringe. The change in free protein concentration (c) in the bulk solution was traced on the chart recorder. When apparent equilibrium was reached, *i.e.* no change in protein concentration in solution, another injection with an increased volume followed, and the differential concentration was recorded. In this manner an adsorption isotherm was constructed over a range of protein concentrations and, simultaneously, the kinetics of adsorption could be followed at each point along the equilibrium isotherm.

By using the stirred tank no problems were encountered with most of the stationary phases as long as particle sizes were above 32 μ m. When smaller particles were employed, clogging of the filter occurred, leading to a decrease in the flow-rate. Air bubbles were formed due to cavitation, and this resulted in some experiments being terminated prior to the determination of adsorption data at high concentration ranges. Spherosil and also the Fractogel supports very often gave a similar problem, but the reason was found to be the presence of either very small particles or other contaminants in the gel. In general, most difficulties were encountered with silica-based or non-porous glass beads, where microparticles very quickly accumulated at the filter. These difficulties restricted the use to silicas with diameters > 25 μ m in the stirred tank, and kinetic data were obtained only for the Spherosil and non-porous glass bead supports of larger particle diameter.

Procedure for equilibrium experiments

An alternative method of batch adsorption was utilized to circumvent the problems experienced with the stirred-tank system described above and to compare data obtained from the stirred tank. By using 10 tubes with a maximum capacity of 5 ml, 0.1 g of the affinity sorbent, varying protein and buffer solutions, adjusted to a final volume of 2 ml, were added such that the same ratios as in the method above were maintained. The flasks were shaken in a water bath for 2 h to simulate a state of equilibrium. The amount of protein adsorbed on the gel was then determined from the difference in concentration initially added to that found in the supernatant afterwards.

Evaluation of thermodynamic data

The amounts of adsorbed protein (q^*) at equilibrium from either stirred-tank or equilibrium experiments were plotted against the free protein concentration, c^* , in solution (*cf.* Figs. 2 and 3). In the case of HSA, the c^* value was corrected for 6% impurities in the HSA preparation, which were found not to bind to the Cibacron Blue

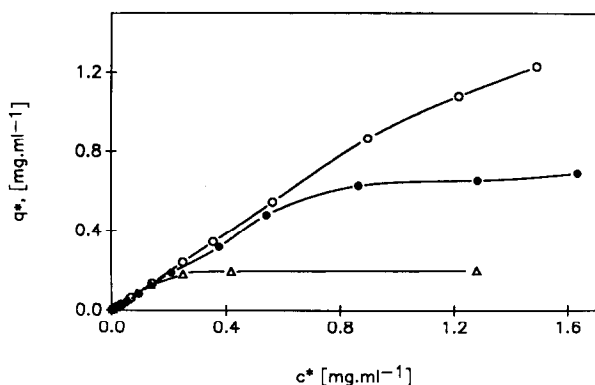


Fig. 2. Equilibrium isotherms for the adsorption of lysozyme onto three different pore size Fractogel TSK HW immobilized Cibacron Blue F3GA. An amount of 1 g of wet gel was suspended in 20 ml of 50 mM Tris · HCl pH 7.8, temperature 318.5 K. (○) Fractogel HW 55 (S), (●) Fractogel HW 65 (F), (△) Fractogel HW 75 (F).

F3GA-immobilized sorbents from corresponding frontal analysis experiments. Each experiment was terminated after the system approached saturation (upper part of the isotherm). For the determination of the accessible ligand concentration (q_m) and the dissociation constant (K_d) a double reciprocal plot of $1/q^*$ against $1/c^*$ was chosen. This numerical approach permits q_m to be evaluated from the y -intercept and K_d from the slope of the linear part of the plot, as illustrated in Fig. 4. Additionally, a plot of c^*/q^* against c^* was made to assure that the data selected for the determination of the thermodynamic parameters were appropriate. This could not always be achieved from the double reciprocal plot due to the reciprocal relationship to the concentration. A Scatchard plot analysis³³, *i.e.* plotting q^*/c^* against adsorbed protein q^* (*cf.* Fig. 5) completed this analysis. Due to the sensitivity of the Scatchard plot, different types of interaction could be discerned, mainly non-specific and specific interactions, and protein-protein association, the latter interaction often occurring during protein adsorption.

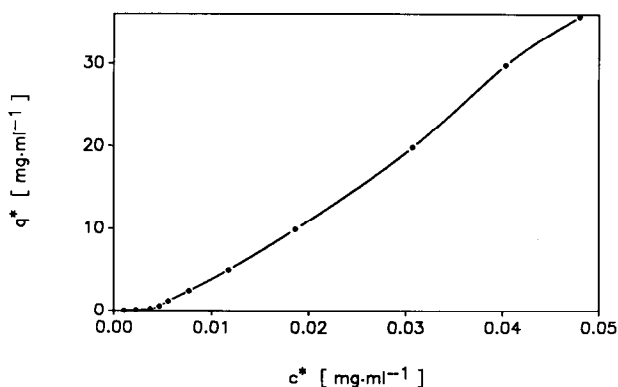


Fig. 3. S-shaped isotherm from adsorption of lysozyme to Cibacron Blue F3GA immobilized to Trisacryl GF 2000. An amount of 1 g of wet gel was suspended in 50 mM Tris · HCl pH 7.8, temperature 318.5 K.

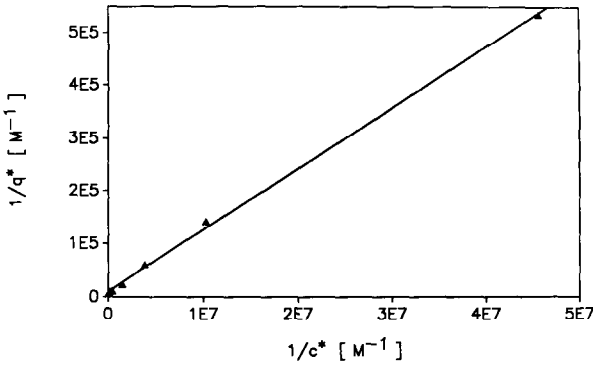


Fig. 4. Double reciprocal plot from the adsorption of HSA to Blue Sepharose CL6B in 50 mM Tris · HCl pH 7.8, temperature 318.5 K.

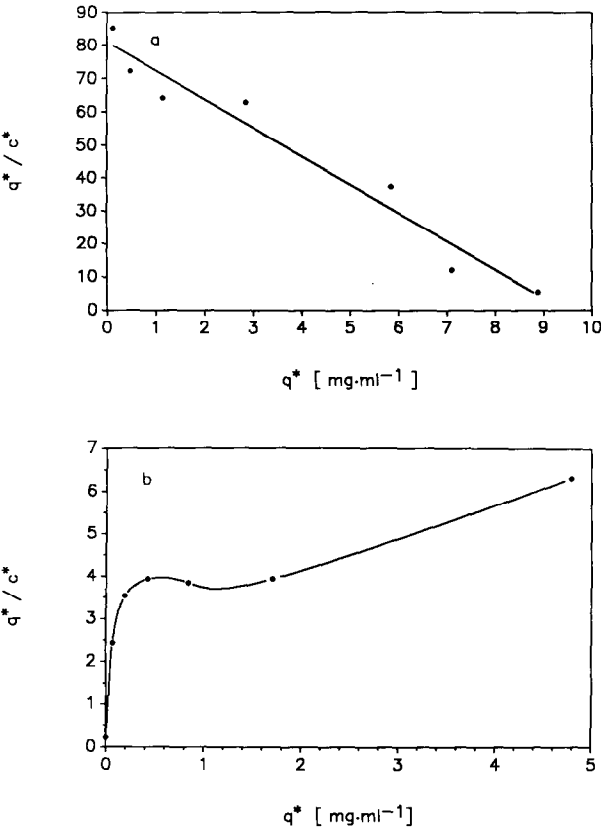


Fig. 5. Scatchard plot analysis derived from adsorption data of the Blue Sepharose CL6B support. (a) HSA adsorption, the observed linearity confirms a specific interaction as expected. (b) Lysozyme adsorption, the increase in protein adsorption at higher protein concentration arises from protein-protein interaction.

Evaluation of equilibrium times

The evaluation of kinetic data was mainly based on comparison of the kinetic uptake of the different proteins by the affinity sorbents. In addition, the periods of time between injection and equilibrium in the stirred-tank experiment at $10 \pm 5\%$ and at $60 \pm 10\%$ of saturation were measured for each affinity sorbent and protein, as displayed

TABLE III
CHARACTERISTIC PARAMETERS OF AFFINITY SORBENTS

Sorbent	q_m (mol/ml)	K_d (M)	Equilibration time (min)	
			$10 \pm 5\%$ of saturation	$60 \pm 10\%$ of saturation
Trisacryl GF 2000				
HSA ^a	$2.3 \cdot 10^{-8}$	$2.8 \cdot 10^{-7}$	8	22
HSA ^b	$7.8 \cdot 10^{-8}$	$1.0 \cdot 10^{-6}$	12	40
HSA (+ NaCl)	$6.4 \cdot 10^{-8}$	$2.1 \cdot 10^{-6}$	—	20
Lysozyme ^a	$9.4 \cdot 10^{-6}$	$6.3 \cdot 10^{-6}$	3.4	20
Lysozyme ^b	—	$1.3 \cdot 10^{-5}$	3	20
Lysozyme (+ NaCl)	$4.7 \cdot 10^{-6}$	$1.2 \cdot 10^{-3}$	3	> 8
Sepharose CL6B				
HSA	$4.9 \cdot 10^{-8}$	$5.2 \cdot 10^{-7}$	3.6	10
HSA (+ NaCl)	$6.8 \cdot 10^{-8}$	$7.3 \cdot 10^{-7}$	—	12
HSA ^c	$1.3 \cdot 10^{-7}$	$1.4 \cdot 10^{-6}$	4.5	31
ADH ^c	$4.5 \cdot 10^{-8}$	$5.1 \cdot 10^{-7}$	11	46
Sepharose 4B				
HSA	$6.2 \cdot 10^{-8}$	$5.9 \cdot 10^{-7}$	5	16
Cellufine GC 700				
HSA	$5.8 \cdot 10^{-8}$	$2.7 \cdot 10^{-6}$	14	50
Fractogel HW 55 (S) ^d				
HSA	$4.0 \cdot 10^{-8}$	$7.0 \cdot 10^{-5}$	—	—
Lysozyme	$1.9 \cdot 10^{-7}$	$1.9 \cdot 10^{-4}$	—	—
Fractogel HW 65 (F) ^d				
HSA	$3.0 \cdot 10^{-8}$	$3.8 \cdot 10^{-5}$	> 3	> 7
Lysozyme	$1.2 \cdot 10^{-7}$	$1.4 \cdot 10^{-4}$	> 4	> 8
Fractogel HW 75 (F) ^d				
HSA	$1.0 \cdot 10^{-8}$	$2.8 \cdot 10^{-5}$	> 1.3	> 6
Lysozyme	$6.0 \cdot 10^{-8}$	$7.4 \cdot 10^{-5}$	> 0.1	> 8
Nucleosil 300-2540 ^e				
HSA	$2.9 \cdot 10^{-7}$	$1.4 \cdot 10^{-6}$	> 5	> 40
Glass beads fraction 4				
Lysozyme (+ NaCl)	—	—	~0.5	
Spherosil X0B030				
Lysozyme (+ NaCl)	—	—	> 60	

^a Low density of immobilized Cibacron Blue F3GA.

^b High density of immobilized Cibacron Blue F3GA.

^c Commercial available Blue Sepharose CL6B.

^d Total ligand concentration from differential UV absorbance readings, an overestimate of accessible ligand concentration.

^e Elution of HSA was impossible.

in Table III. This was found to be the most appropriate way to illustrate adsorption characteristics of the various sorbents used in the present study.

RESULTS

Adsorption of lysozyme

Equilibrium constants of the lysozyme–Cibacron Blue F3GA complex were found to be substantially lower than equilibrium constants for HSA, as indicated in Table III. The adsorptive performance of all Fractogel HW-based sorbents was generally lower than that of the Trisacryl-based sorbents when no salt was added to the buffer. In Fig. 2 the equilibrium isotherms of the adsorption of lysozyme on three Fractogel-based sorbents HW 55 (S), HW 65 (F) and HW 75 (F) are displayed. The Fractogel HW 55 sorbent demonstrated the greatest capacity. This is consistent with the smaller pore size and corresponding higher surface area of this sorbent compared to the other sorbents. The data obtained with the Fractogel HW 55 dye sorbent from the two methods used, as described in the Experimental section, gave remarkably concordant results, and the calculated isotherms reflected this. However, a crucial point of difference was the leakage characteristics of adsorbed dye molecules which did not bind to the sorbent during the immobilization procedure. With the salt concentration finally chosen for the immobilization conditions (0.5 *M* NaCl), the coupling and washing supernatants contained very little free dye after removal of the dye sorbent by filtration, indicating that either very strong chemical immobilization or physical adsorption of the dye molecules had occurred. When no salt in the washing procedure was employed, most of the physically adsorbed dye was eluted. Nevertheless, when these sorbents were exposed to protein for the first time, more dye molecules were displaced by the adsorbing proteins, as evident from higher UV absorption readings of the effluent than theoretically was possible. The displacement of the dye decreased after incubation of these sorbents with protein solution and subsequent reconditioning prior to the next experiment, but it was never eliminated entirely throughout the experimental series with the Fractogel HW sorbents. In the case of the Trisacryl affinity sorbents no such dye displacement was evident. However, the curve of the equilibrium isotherm for lysozyme with the Trisacryl GF2000 dye sorbent was S-shaped, as indicated in Fig. 3. This result was reproducible with different batches of the Trisacryl GF2000 dye sorbent in subsequent experiments under the same eluent conditions. In other experiments, when 0.5 *M* NaCl was added to the buffer no S-shaped isotherm was observed but rather a linear isotherm, which did not curve downward at higher concentrations. The observed equilibrium constant for lysozyme with the Trisacryl GF2000 dye sorbent in the presence of 0.5 *M* NaCl of 847 *M*⁻¹ was much lower than that obtained from experiments without salt, indicating that added salt decreases the Cibacron Blue–lysozyme interaction dramatically.

At low concentrations, all the transformed isotherm data from different sorbents deviated in the double reciprocal plots from linearity, suggesting that the Langmuir isotherm model is not wholly indicative of the experimental situation. As previously mentioned, the derivation of the simplest form of the Langmuirean equation assumed specific binding and homogeneity of the sorbent. Participation of other phenomena subverting the role of these two important factors may account for this deviation from linearity with the double reciprocal plot. Finally, Scatchard plot analysis indicated that

other mechanisms of interaction are present, as demonstrated by Fig. 5a. For example, at high protein concentrations, lysozyme appeared to have a higher affinity for the dye sorbent, a situation which can only be attributed to protein-protein interaction, exacerbated when lysozyme is dissolved at a pH higher than 8.0³⁴. Self association of lysozyme at pH 7.8 might also occur at the surface of the affinity sorbent where locally a higher protein concentration is achieved. The same behaviour in the Scatchard plot was manifested when salt was added to the buffer, although in this case it developed at low protein concentrations. The latter effect confirmed that protein-protein association was an important component of the increased interaction of these proteins at higher salt concentration. The observed equilibrium constant with 0.5 M NaCl may be related to the dimerisation equilibrium constant of lysozyme at pH 7.8.

Adsorption of HSA

Compared to lysozyme, HSA displayed a much higher affinity to Cibacron Blue, as illustrated in Table III. Equilibrium isotherms demonstrated normal behaviour, as shown in Fig. 6 for the Trisacryl- and Sepharose-immobilized dye sorbents. In the case of the Cellufine GC 700 sorbent, dye displacement was evident at low protein concentrations, and this leakage behaviour could not be changed by preadsorption of the gel with HSA, as described for lysozyme with the Fractogel affinity sorbents. With the Cellufine GC 200 sorbent the adsorbed dye was readily released in the absence of protein, indicating that significant amounts of dye were physically adsorbed in the pores of the gel. HSA, adsorbed on silica-immobilized Cibacron Blue F3GA, could not be adequately eluted under any elution condition applied. However, the adsorption did not appear to be irreversible, since apparent equilibrium binding was observed after each protein injection. As described for Cellufine GC 700, the silica-based Nucleosil 300-2540 sorbent also displayed dye displacement at low protein concentration.

Despite interference of dye displacement of affinity sorbents with the adsorbate HSA, double reciprocal plots and Scatchard plot analysis of the experimental data suggested the absence of nonspecific interactions, that is, a linear relationship between

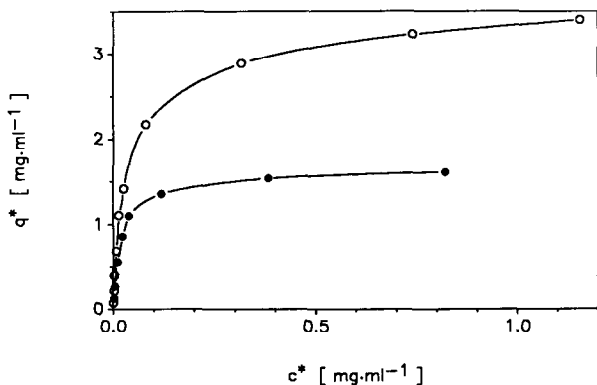


Fig. 6. Langmuirian isotherms for the adsorption of HSA to Cibacron Blue F3GA immobilized supports. An amount of 1 g of wet gel was suspended in 50 mM Tris · HCl pH 7.8, temperature 318.5 K. (○) Sepharose CL6B, (●) Trisacryl GF 2000.

the transformed parameters c^* and q^* was observed. Deviations from linearity in the adsorption isotherm at low protein concentrations was always associated with dye displacement, which was evident as high UV absorption readings of the eluent stream. HSA displayed lower affinity for the immobilized dye when 0.5 M NaCl was present in the buffer, a result which agrees with those observed for the adsorption of lysozyme in the presence and absence of salt. However, the differences in association affinities were less dramatic (*cf.* Table III). In the case of the Trisacryl GF 2000 dye affinity sorbent, the calculated q_m values are identical for experiments carried out in the presence and absence of 0.5 M NaCl. However, when the Sepharose CL6B dye affinity sorbent was employed, a 40% increase in q_m was observed when 0.5 M NaCl was added.

The behaviour of the Fractogel sorbent diverged from the other affinity sorbents, displaying only very little adsorption capacity and also low equilibrium constants with HSA. This behaviour may have been a consequence of the shrinkage of the Fractogel sorbent during immobilization or of a change in its microstructure and fractal surface, effects which could be responsible for low protein accessibilities to the immobilized Cibacron Blue F3GA. A change in the microstructure of the Fractogel sorbents was found in our previous experiments, in which carbonyldiimidazole (CDI) activation had been used and where an increase in ligand density on Fractogel HW 65 resulted in only a modest increase in capacity but a significant decrease in the proportion of high-affinity sites accessible to the substrate³⁵.

Adsorption of ADH

In contrast to results reported in the literature on ADH binding to Cibacron Blue F3GA³⁶, ADH from yeast did not bind to any of the Cibacron Blue F3GA-immobilized soft gels or silica sorbents. This result was unexpected in light of our earlier studies that demonstrated that silica-immobilized Cibacron Blue F3GA binds lactate dehydrogenase (LDH) and malate dehydrogenase in a very specific mode²⁴. ADH, like other dehydrogenases, requires NADH as a cofactor, and in a manner analogous to other NADH-dependent enzymes, this enzyme should bind to Cibacron Blue F3GA via the enzyme active site, since the dye is reported to mimic the cofactor NADH³⁷. However, the lack of binding of ADH suggests that the adsorption mechanism of this enzyme is different from that of the other dehydrogenases. To verify the binding of LDH to Cibacron Blue F3GA immobilized on soft gels, Trisacryl GF 2000 was chosen as an alternative dye affinity sorbent and LDH was adsorbed on and eluted from this sorbent, confirming the results of our previous work. Commercially available Blue Sepharose CL6B was also chosen for ADH adsorption to examine the influence of dye purity, as detrimental effects due to dye heterogeneity of commercial dyes could influence the experimental outcome. In this case, high affinity of the enzyme for the dye sorbent was demonstrated. Our results, showing no binding of ADH to the other dye sorbents, can be explained if the Cibacron Blue F3GA obtained from Serva contained only the *meta*-substituted isomer at the terminal benzene ring, a compound which is reported not to bind to ADH³⁸.

The affinity constant of ADH binding to Blue Sepharose CL6B was comparable to the observed affinity constant of HSA for Cibacron Blue F3GA, despite the requirement for ADH to be eluted by using 0.5 M NaCl in the buffer. These results suggest that binding of ADH to the dye affinity sorbent is mainly due to ionic interaction and hydrogen-bonding sites, whereas HSA binds also via complementary

hydrophobic binding moieties on the protein and the ligand, where the affinity can only be moderated by addition of salt to the buffer system. To compare the affinity of ADH and HSA for the same affinity sorbent, HSA was also adsorbed on commercially available Blue Sepharose CL6B, by using the same buffer conditions. The results from this experiment showed that the affinity of ADH is twice as high as that of HSA, while the accessibility of protein for the dye affinity ligand is only one-third as large. This behaviour is in accord with the size difference between ADH and HSA which will restrict to a significant extent the diffusion of ADH to the ligand immobilized in narrow pores.

Diffusion properties of the proteins

A dramatic difference in adsorption behaviour is evident when the protein uptake in the bath system for proteins of increasing molecular weights are compared, using the same affinity sorbent. Whilst equilibrium of lysozyme was usually attained with the experimental system between 2 and 5 min, equilibration times for HSA, were 2–3 times longer and for ADH slightly longer than for HSA. Especially at low ADH concentrations, the time required for equilibrium to be accomplished was much longer than for lysozyme and HSA, a result which suggests that ADH binding is mainly diffusion controlled.

Mass-transfer restrictions of affinity sorbents

Equilibration times after injection of protein solution into the stirred tank varied substantially with the extent of saturation of the affinity sorbent. At low adsorption concentration (q^*) the kinetics appeared to be very fast and not controlled by the diffusion of the protein into the porous system of the sorbent (Fig. 7). At this stage, most of the protein is immediately adsorbed on the external surface and the outer shell of the affinity sorbent. Under these conditions, pore diffusion is negligible, if not absent, and has very little influence on the adsorption rate. At higher protein concentrations in the bath experiments, when the affinity sorbent is close to saturation, protein uptake decreased dramatically. This is in concordance with eqn. 2, and dq/dt will reduce as q approaches q_m and also the dissociation of adsorbed protein from the sorbent becomes more noticeable close to saturation. The decrease in protein uptake at these protein concentrations was more noticeable when supports with low permeability ranges were used, like Cellufine GC 700 or Nucleosil 300-2540. This may indicate that steric restrictions at pore entrances and/or inside the porous system of these sorbents may be a major rate-determining step when the protein size to pore size ratio, λ , is greater than 0.2, as suggested by Webster¹⁴. Upon saturation of the affinity sorbent, only a small amount of protein is adsorbed and the steady state is very quickly attained again. This trend was consistently evident in the results from all sorbents and proteins used in this study.

Protein uptake in the bath experiments decreased with increased particle size due to longer diffusion paths, as expected. For the non-porous glass bead affinity sorbents, equilibration times were in the range of 20–35 s, compared to 10–40 min for the porous gel affinity sorbents. The non-porous glass affinity sorbents also demonstrated a second, slower step, which was probably a consequence of the high degree of polymerization that took place during the activation step when the silane was covalently linked to the glass surface. Surprisingly, the Nucleosil 300-2540 sorbent

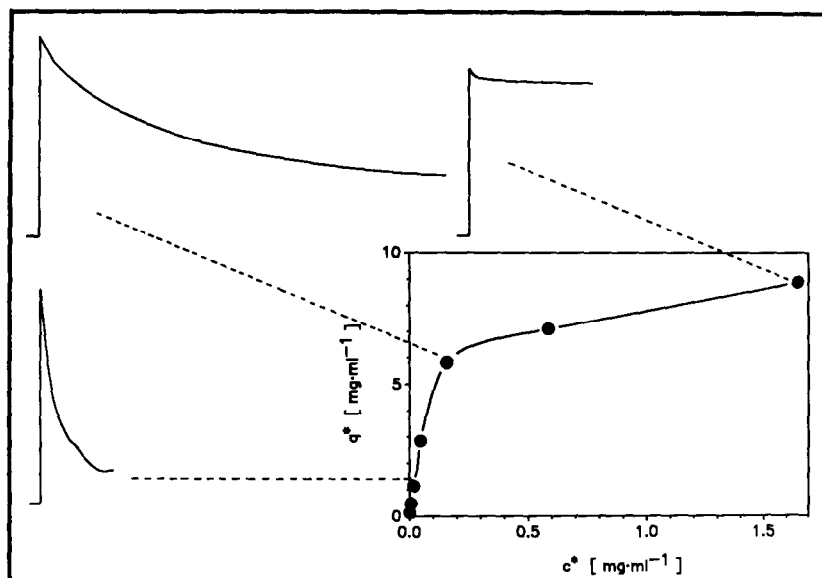


Fig. 7. Experimental kinetic profiles during adsorption of HSA onto Blue Sepharose CL6B for different saturation levels corresponding to data points on the given isotherm.

displayed also slow adsorption kinetics. In this case, pore-size restrictions may influence the adsorption time more dramatically than the particle size. In comparison to the Trisacryl and Sepharose affinity sorbents, which demonstrated the fastest kinetics, the Nucleosil affinity sorbent has a smaller particle size, as shown in Table II. Another explanation for the slow adsorption kinetics of this sorbent could be based on an adsorption mechanism different from that for the soft gel affinity sorbents. The fact that elution of bound HSA from Nucleosil 300 silica-immobilized Cibacron Blue F3GA was not successful points to this possibility. When Spherosil (average particle size of 200 μm) was employed to adsorb lysozyme, equilibrium could not be achieved after more than 40 min. This may indicate that this silica-based sorbent has a relatively high amount of small pore entrances compared to the actual pore size, or that polymerization of the silane used for the modification of this support caused cross-linkage. Both effects would make it difficult for the protein to find its way to the centre of each particle.

DISCUSSION

As demonstrated in this study, the stirred-tank experiments have been found useful to display the characteristics of the affinity system, including information about diffusion restrictions of the affinity sorbents. An alternative way to obtain thermodynamic data is frontal analysis³⁹, but the experimental set-up is more complicated and the accumulation of data can be a very time-consuming process (e.g. low flow-rates need to be used when gels with large particle size are chosen as typically required for large-scale purifications) and processing of thermodynamic data obtained from breakthrough curves is tedious work, requiring high precision when done

manually. Furthermore, no kinetic data can be directly derived from breakthrough curves. Differences in diffusion restrictions can only be detected by comparison of the shape of the curves for different supports. In the finite bath experiment, however, both thermodynamic and kinetic data can be obtained simultaneously. In our experience, two experiments can be conveniently performed per day, yielding most of the data needed to describe the affinity system. Furthermore, systems with relatively low equilibrium constants ($K_a = 200$) can be investigated, a situation which makes data processing rather difficult when frontal analysis is utilized. In such circumstances the difference between retention volume V_e and V_o in frontal chromatograms becomes very small and subject to significant errors when small column volumes are employed.

Dye displacement from Fractogels and silica-based affinity sorbents were demonstrated even at very low protein levels due to measured UV absorption readings higher than those achieved when all of the injected protein remained unbound. This situation is often not realized in column experiments, as non-binding contaminants in the protein solution, applied to the column, can result in an increase in UV absorption readings, commencing at V_o . Displacement of dye in column experiments can result in the dye being eluted slowly from the column. In such column experiments, it is not possible to distinguish between adsorption due to contaminants or the dye. However, the detection of even low dye levels that leak from either physically adsorbed sites or weak chemically linked sites within the structure of the gel matrix is important for quantitation before scale-up is performed. The released dye must be removed from the final product if a pharmaceutical product is to be manufactured. Furthermore, the progressive loss of dye from the stationary phase will influence the capacity.

The low capacity and affinity of the Fractogel-based dye sorbents is indicative of a change of the gel structure occurring during the immobilization of Cibacron Blue F3GA, despite the fact that this support is more rigid than the other soft gels used in this study. Structural changes have been previously reported with Fractogel sorbents after using CDI activation³⁵. A change in the gel structure may be explained by hydrophobic interaction of the dye with the matrix leading to pore compression. This was indicated by the adsorption of non-bound dye molecules at high salt concentrations. If strong hydrophobic interaction of adsorbed dye molecules with the matrix network takes place, the fractal surface of the matrix will change, trapping also some dye molecules inside the tortuous and cul-de-sac surface pockets that may have formed around the dyes. Hydrophobic interactions may have additionally caused some change in the arrangement of cross-linkage of polymeric chains which could freely move inside the porous system and accommodate proteins before immobilization. The participation of very strongly adsorbed dye in this physical environment would also explain dye displacement during protein adsorption. During adsorption of lysozyme on Fractogel HW 65 at low protein concentration, dye displacement is particularly apparent, equilibrium times before the steady state is reached being at least 3–4 times higher than the equilibration times shown in Table III. The long equilibration times may be a consequence of the movement of lysozyme through the network of polymer chains and the release of adsorbed dye molecules that have formed connections between chains and are trapped inside the pore pockets. This dye displacement phenomenon was less evident in a subsequent experiment and even less apparent after batch incubation with lysozyme for 24 h. When the Fractogel sorbent is used for adsorption of HSA, only a small amount of dye ligands are accessible for protein binding and/or

dye displacement. This observation suggests that the accessibility of the dye ligand is restricted to interaction with either the outer shell or with a limited portion of the geometrical surface of the affinity sorbent. The above observation may be due to the high ligand densities intentionally used and might have been less significant if lower ligand densities had been utilized.

The difficulty of eluting HSA from silica-immobilized dye sorbents is probably due to protein reorientation close to the silica surface. This behaviour consequently leads to irreversible adsorption at either the silica surface itself or at the immobilized ligand, caused by the high immobilization level achieved with the silica sorbent (see Table III). An alternative possibility which must be considered involves the influence of the chaotropic salt potassium thiocyanate used for protein elution. This reagent changes the tertiary structure of proteins, due to alteration of the solvent sphere, and this may expose further sites on the protein for interaction with the dye. These desorption difficulties cannot be explained by irreversible interaction between the protein and the dye during the adsorption step. If irreversible adsorption was always taking place, complete adsorption of HSA would have been achieved until saturation of the affinity sorbent was accomplished, a situation which was not observed experimentally.

Dissociation constants of lysozyme with Trisacryl-immobilized Cibacron Blue F3GA in the absence of salt were in the same range as reported by Chase⁵. The dissociation constant of all Fractogel sorbents was approximately an order of magnitude higher, representing lower affinity interactions. If it is assumed that the same interaction mode occurs between lysozyme and all sorbents used in this study, the dissociation constant should not vary by this magnitude. The observed differences demonstrated that the total capacity, as displayed in Table III for the Fractogel sorbents, does not represent the accessible capacity, q_m , of these sorbents. Because the total capacities were calculated from differential UV absorbance readings before and after coupling of the ligand, they represent an overestimation of the accessible ligand concentration.

Differences in the kinetics between the soft-gel- and silica-based affinity sorbents used in this study demonstrated also distinctive differences in pore diffusion restrictions. Soft-gel supports are considered to be based on an open network system in which the gel is formed and stabilised by cross linkage of this flexible network. Silica-based supports are mainly based on a pore system that cannot be changed by pressure or drag forces. The observed slow kinetics during adsorption of HSA to Nucleosil 300-2540 reflect the high value for λ (0.28). Under these circumstances high diffusion restrictions will occur when saturation of the affinity sorbent is nearly accomplished. The slow kinetics for Cellufine GC 700 are probably also based on a high protein size to pore size ratio, because the unchanged native support accommodates proteins up to a molecular weight of 400 000 daltons. Comparing Trisacryl or Sepharose affinity sorbents with Nucleosil 300, the effective value of λ of the soft gels must be much smaller according to the faster kinetics observed with these sorbents. It appears that among all the sorbents used in this study, Trisacryl and Sepharose had the best characteristics in terms of low non-specific interactions and rapid kinetics.

The observation that equilibration times increase as sorbent saturation is approached and when sorbents with small pore sizes are employed, clearly demonstrate that the assumption of local equilibrium is invalid. Furthermore, mass-transfer

restrictions cannot be ignored and could well be the major adsorption rate-determining factor, particularly when sorbents based on Cellufine GC 700 or Nucleosil 300-2540 for the adsorption of HSA are used, where high protein size to particle size ratios occur. When such sorbents are utilized, mass transfer restrictions change dramatically after the protein has been adsorbed at the outer surface. For example, the value of λ increases from 0.28 to approximately 0.6 based on a diameter of HSA of 8.35 nm and assuming a monolayer of adsorbed proteins in the first stage. Therefore, adsorption kinetics will be controlled much more by diffusion restrictions as well as the reverse reaction rate constant (*cf.* eqn. 2), since protein dissociation from the sorbent at pore constrictions will contribute to the adsorption kinetics throughout the adsorption process. It has been found that equilibration times as presented in Table III for the adsorption of HSA, which are measured from injections at increasing saturation levels, represent a very practical way to compare affinity sorbents of different pore and particle characteristics since they do not require sophisticated computer programs for the calculation of kinetic and diffusion parameters. However, equilibration times are representative for the described affinity systems only because the adsorption depends upon a large number of factors as mentioned above. If information is needed to calculate and predict the behaviour of batch adsorption in large batches for industrial purposes, then discrimination of the pore diffusivity and the film mass-transfer coefficient from the overall reaction rate is recommended⁴⁰. To validate the protocols proposed in these investigations, further detailed analysis of sorbents with different surface characteristics is currently underway in this laboratory, including studies with strong ion exchangers where rectangular equilibrium isotherms may be observed⁴¹.

ACKNOWLEDGEMENT

The support of the Australian Research Grants Committee & Monash University Special Research Grants is gratefully acknowledged. F.B.A. is a recipient of a Monash University Postdoctoral Fellowship.

REFERENCES

- 1 A. W. Purcell, M. I. Aguilar and M. T. W. Hearn, *J. Chromatogr.*, 476 (1989) 125.
- 2 R. R. Walters, *Anal. Chem.*, 57 (1985) 1099.
- 3 E. Boschetti, J. M. Egly and M. Monsigny, *Trends Anal. Chem.*, 5 (1986) 4.
- 4 F. H. Arnold, H. W. Blanch and C. R. Wilke, *Chem. Eng. J.*, 30 (1985) 25.
- 5 H. A. Chase, *J. Chromatogr.*, 297 (1984) 179.
- 6 R. M. Moore and R. R. Walters, *J. Chromatogr.*, 384 (1986) 53.
- 7 Cs. Horváth and J.-M. Engasser, *Biotechnol. Bioeng.*, 16 (1974) 900.
- 8 L. Goldstein, *Methods Enzymol.*, 44 (1976) 397.
- 9 H. Poppe and J. C. Kraak, *J. Chromatogr.*, 255 (1983) 395.
- 10 M. T. W. Hearn, in S. Asenjo (Editor), *Industrial applications of Biotechnology*, Marcel Dekker, New York, 1989, pp. 140–165.
- 11 F. H. Arnold, H. W. Blanch and C. R. Wilke, *J. Chromatogr.*, 355 (1986) 1.
- 12 I. Langmuir, *J. Am. Chem. Soc.*, 38 (1916) 2221.
- 13 M. E. Young, P. A. Carroad and R. L. Bell, *Biotechnol. Bioeng.*, 22 (1980) 947.
- 14 I. A. Webster, *Biotechnol. Bioeng.*, 25 (1983) 2479.
- 15 M. T. W. Hearn, M. Aguilar and A. Hodder, *J. Chromatogr.*, 458 (1988) 45.
- 16 M. T. W. Hearn, in J. C. Janson (Editor), *High Resolution Purification of Proteins*, VCH Press, FL, 1988 in press.

- 17 D. M. Smith, *AIChE J.*, 32 (1986) 1039.
- 18 R. L. Fournier, *AIChE J.*, 32 (1986) 1036.
- 19 W. W. Yau, J. J. Kirkland and D. D. Bly, *Modern Size Exclusion Chromatography*, Wiley, New York, 1979.
- 20 D. A. P. Small, T. Atkinson and C. Lowe, *J. Chromatogr.*, 216 (1981) 175.
- 21 P. G. H. Byfield, S. Copping and R. L. Himsworth, *Mol. Immunol.*, 21 (1984) 647.
- 22 E. Gianazza and P. Arnaud, *Biochem. J.*, 201 (1982) 129.
- 23 C. R. Lowe, S. J. Burton, J. C. Pearson and Y. D. Clonis, *J. Chromatogr.*, 376 (1986) 121.
- 24 F. B. Anspach, K. K. Unger, J. D. Davies and M. T. W. Hearn, *J. Chromatogr.*, 457 (1988) 195.
- 25 F. B. Anspach, H.-J. Wirth, K. K. Unger, P. Stanton, J. R. Davies and M. T. W. Hearn, *Anal. Biochem.*, (1989) in press.
- 26 F. B. Anspach, K. K. Unger, H. Giesche and M. T. W. Hearn, *4th International Symposium on HPLC of Proteins, Peptides, and Polynucleotides*, Baltimore, MD, 1984, paper No. 103.
- 27 A. I. Liapis, F. B. Anspach, M. E. Findley, J. Davies, M. T. W. Hearn and K. K. Unger, *Biotechnol. Bioeng.*, (1989) in press.
- 28 P. Wikström and P.-O. Larsson, *J. Chromatogr.*, 388 (1987) 123.
- 29 F. E. Regnier and R. Noel, *J. Chromatogr. Sci.*, 14 (1976) 316.
- 30 D. Hanggi and P. Carr, *Anal. Biochem.*, 149 (1985) 91.
- 31 D. A. P. Small, T. Atkinson and C. R. Lowe, *J. Chromatogr.*, 266 (1983) 151.
- 32 *Gel Filtration Theory and Practice —Laboratory Handbook*, Pharmacia, Uppsala, 1985.
- 33 J. R. Sportsman and G. S. Wilson, *Anal. Chem.*, 52 (1980) 2013.
- 34 P. R. Wills, L. W. Nichol and R. J. Siezen, *Biophys. Chem.*, 11 (1980) 71.
- 35 M. T. W. Hearn, *J. Chromatogr.*, 376 (1986) 245.
- 36 Y. C. Liu and E. Stellwagen, *J. Chromatogr.*, 376 (1986) 149.
- 37 D. A. P. Small, T. Atkinson and C. Lowe, *J. Chromatogr.*, 216 (1981) 175.
- 38 J. F. Biellmann, J. P. Samama, C. I. Brandon and H. Eklund, *Eur. J. Biochem.*, 102 (1979) 107.
- 39 K.-I. Kasai, Y. Oda, M. Nishikata and S.-I. Ishi, *J. Chromatogr.*, 376 (1986) 33.
- 40 B. H. Arve and A. T. Liapis, *AIChE J.*, 33 (1987) 179.
- 41 A. Velayudhan and Cs. Horváth, *J. Chromatogr.*, 443 (1988) 13.
- 42 J. Janin, *Nature (London)*, 277 (1976) 491.
- 43 R. C. Travers and F. C. Church, *Int. J. Pept. Protein Res.*, 26 (1985) 539.